International Research Institute/Applied Research Centers (IRI/ARCs) regional model intercomparison over South America

J. Roads,[1] S. Chen,[1] S. Cocke,[2] L. Druyan,[3] M. Fulakeza,[3] T. LaRow,[2] P. Lonergan,[3] J.-H. Qian,[4] and S. Zebiak[4]

Received 20 November 2002; revised 14 March 2003; accepted 20 March 2003; published 29 July 2003.

[1] A regional modeling intercomparison project for South America among the (1) Scripps Experimental Climate Prediction Center regional spectral model (RSM), (2) Florida State University nested regional spectral model (FSUNRSM), (3) Goddard Institute for Space Studies regional climate model (RCM), and (4) IRI regional climate model (RegCM2) is described herein. All regional models were driven by the NCEP/NCAR I global reanalysis over a South American domain centered on Brazil. In comparison to new Xie and Arkin 0.5° land observations, the regional models had a seasonal systematic precipitation error that was somewhat similar to the driving NCEP/NCAR reanalysis systematic error, although the regional model ensemble mean error was somewhat smaller, indicating a potential value for using multiple model ensembles. However, correlations, threat scores and biases were not noticeably better. In short, at their current levels of skill, regional models do not yet provide a noticable improvement over large-scale analyses. *INDEX TERMS:* 3309 Meteorology and Atmospheric Dynamics: Climatology (1620); 3337 Meteorology and Atmospheric Dynamics: Numerical modeling and data assimilation; 3319 Meteorology and Atmospheric Dynamics: General circulation; *KEYWORDS:* Regional climate modeling, Brazil, South America

Citation: Roads, J., S. Chen, S. Cocke, L. Druyan, M. Fulakeza, T. LaRow, P. Lonergan, J.-H. Qian, and S. Zebiak, International Research Institute/Applied Research Centers (IRI/ARCs) regional model intercomparison over South America, *J. Geophys. Res.*, *108*(D14), 4425, doi:10.1029/2002JD003201, 2003.

1. Introduction

[2] At the end of 1999, the International Research Institute (IRI) and a few of the NOAA Applied Research Centers (ARCS), began a community regional modeling intercomparison project with the goal of assessing the capabilities and readiness of various regional climate models to eventually downscale IRI global forecasts. This intercomparison project was open to the community but despite the initial interest by a large number of outside participants, only a few groups wound up finishing the comparison. This intercomparison should thus be thought of as representative but not fully inclusive of the range of possible simulations that current regional climate models might provide for this region. Besides the IRI, participating ARCS included: Scripps Institution of Oceanography Experimental Climate Prediction Center (ECPC); Florida State Univ. Cooperative Ocean Atmosphere Project (COAPS); and the Goddard Institute for Space Studies (GISS).

[3] Although a number of the regional models taking part in the intercomparison had previously focused upon the US [e.g., *Chen et al.*, 1999; *Roads and Chen*, 2000; *Roads et al.*, 2003], and two (the ECPC RSM and NCAR RegCM2) had participated in the previous US Project for Intercomparison of Regional Climate Simulations (PIRCS [*Tackle et al.*, 1999]), it was felt that a comparison of regional climate models over South America offered a prime opportunity to compare these regional models in a new environment where the IRI was making skillful forecasts with global models comparable to statistical and empirical forecasts [e.g., *Hastenrath and Heller*, 1977; *Hastenrath and Grieschar*, 1993], presumably due to the strong ENSO response in that region [*Ropelewski and Halpert*, 1987] and the additional response to Atlantic SSTs [e.g., *Uvo et al.*, 1998]. The IRI was also working with groups in Brazil to downscale these global forecasts [e.g., *Nobre et al.*, 2001] and there had been a number of previously successful regional simulations of South American climate [e.g., *Horel et al.*, 1994]. Transferability of regional climate models has also been recommended by the Global Energy and Water-Cycle Experiment (GEWEX); since so many of the GEWEX Continental Scale Experiments have focused on developing regional models for specific regions and GEWEX and the developing World Climate Research Program Coordinated Enhanced Observing Period project now want to test these

[1] Experimental Climate Prediction Center, Scripps Institution of Oceanography, University of California, San Diego, La Jolla, California, USA.
[2] COAPS, Florida State University, Tallahassee, Florida, USA.
[3] Earth Institute at Columbia University and NASA/Goddard Institute for Space Studies, New York, New York, USA.
[4] International Research Institute, Lamont-Doherty Earth Observatory, Columbia University, Palisades, New York, USA.

0148-0227/03/2002JD003201$09.00

Table 1. Regional Model Characteristics

Model	Reanalysis	Scripps RSM	FSUNRSM	GISS RCM	IRI RegCM2
Levels	28	28	27	16	14
Type	spectral	spectral	spectral	grid	grid
SW. Rad.	*Lacis and Hansen* [1974]	*Chou and Lee* [1996]	CCM 3.6 [*Kiehl et al.*, 1998a, 1998b]	*Davies* [1982]	CCM 3.3 [*Kiehl et al.*, 1998a, 1998b]
LW Rad.	GFDL [*Schwarzkopf and Fels.*, 1991]	GFDL [*Schwarzkopf and Fels.*, 1991]	CCM 3.6 [*Kiehl et al.*, 1998a, 1998b]	*Harshvardhan and Corsetti* [1984]	CCM 3.6 [*Kiehl et al.*, 1998a, 1998b]
Convective Parameterization	SAS [*Kalnay et al.*, 1996]	SAS[a] [*Hong and Pan*, 1996]	*Zhang and McFarlane* [1995]	modified Kuo [*Krishnamurti et al.*, 1990]	*Grell* [1993]
PBL	*Louis et al.* [1982]	*Hong and Pan* [1996]	*Holtslag and Boville* [1993]	[*Krishnamurti et al.*, 1990]	*Holtslag et al.* [1990]
Land Surface	NOAA [*Kalnay et al.*, 1996]	NOAA[a] [see *Chen and Roads*, 2002]	FSU [*Cocke and LaRow*, 2000]	*Fulakeza et al.* [2002]	BATS [*Dickinson et al.*, 1993]

[a]Denotes precipitation in the form of snowflakes or flurries.

regional models where they have not explicitly tuned their parameterizations.

[4] There certainly has been much frustration with our inability to adequately simulate and predict regional climate variations with coarse-resolution global general circulation models (GCMs). Regional models have therefore been developed to downscale larger scale simulations and predictions for specific regions [e.g., *Pielke*, 1984; *Perkey*, 1984; *Anthes et al.*, 1989; *Dickinson et al.*, 1989; *Giorgi and Bates*, 1989; *Giorgi et al.*, 1993a, 1993b; *Kida et al.*, 1991; *DiMego et al.*, 1992; *Horel et al.*, 1994; *Hirakuchi and Giorgi*, 1995; *Jones et al.*, 1995; *McGregor and Walsh*, 1994; *Miller and Kim*, 1996; *Soong and Kim*, 1996; *Ji and Vernekar*, 1997; *Chen et al.*, 1999, 2003; *Leung and Ghan*, 1999a, 1999b; *Leung et al.*, 1999; *Roads and Chen*, 2000; *Anderson et al.*, 2000a, 2000b; *Han and Roads*, 2003], it is commonly assumed that the interactions of the regional model with the higher resolution landscape and the higher resolution of gradients used in the computations of physical processes will eventually help us to make better regional simulations and predictions. It should also be noted that besides possible resolution improvements, regional models also provide a regional focus for examining regional variations.

[5] Our goal in this intercomparison project was to determine whether current regional climate models could make possible improvements upon coarse-scale global analyses by providing more realistic coupling with high resolution South American topography and land surface features as well as more realistically represent precipitation processes. This is certainly quite optimistic since the analyses, while based upon all available global data, which is quite sparse in the South American region, provide a strong forcing to regional models. In addition, many of the regional model parameterizations come from global models that have not yet been adequately tuned for higher resolution simulations. As we shall see, while the potential for improvement certainly exists, regional models are not yet capable of significantly improving upon the global analysis.

[6] In the following sections, we first provide brief descriptions of the participating regional climate models (section 2) and the experiment design. Section 3 describes the basic skill measurements and Intercomparison results are provided in section 4. A summary is given in section 5.

2. Regional Models

[7] The regional models, along with the global analysis, are summarized in Table 1. It should be noted that the regional models did have one disadvantage; they were not reinitialized every 6 hours like the reanalysis. Instead they were all initialized once while the only updated forcing came from the NCEP/NCAR I reanalysis lateral boundary conditions. As described by *Roads et al.* [2003] this resulted in some additional error and it was recommended that analysis downscalings should have more frequent updates. J.-H. Qian et al. (Reinitialized versus continuous simulations for regional climate downscaling, manuscript submitted to *Monthly Weather Review*, 2002) also found that downscaling accuracy was improved by reinitializing a regional climate model every ten days.

[8] The study here includes two spectral models (ECPC RSM and FSURSM) and two grid point models (IRI RegCM2 and GISS RCM). All models were run at 50 km resolution (~150 $\times$ 99) although the number of vertical levels varied from 14 to 28. There were a number of different physical parameterizations utilized, which can be traced to the physical parameterizations used in 3 major global models (NCEP, NCAR, UCLA). Further details about the models are provided below and in Table 1.

2.1. ECPC Regional Spectral Model (RSM)

[9] ECPC's regional spectral model was originally developed by *Juang and Kanamitsu* [1994] [see also *Juang et al.*, 1997]. This model was previously used to simulate and analyze regional climate characteristics of precipitation [*Chen et al.*, 1999; *Hong and Leetma*, 1999], low-level winds [*Anderson et al.*, 2000a, 2000b, 2001], Mississippi River Basin water and energy budgets [*Roads and Chen*, 2000], and US climate simulations [*Roads et al.*, 2003; *Han and Roads*, 2003]. The RSM is a regional extension to the National Centers for Environmental Prediction (NCEP) global spectral model (GSM), which became on 10 January 1995, the basic global model used for the NCEP/ National Center for Atmospheric Research (NCAR) reanalysis (see

Kalnay et al. [1996] for a description of the model). The RSM provides an almost seamless transition between the NCEP global spectral model (GSM) and the higher resolution region of interest. Another advantage, according to *Hong and Leetma* [1999], is that the RSM does not have the same restrictions on nesting size that other regional climate models seem to have and smaller nests can be embedded within the large-scale reanalysis without noticable errors or influences. Basically, the RSM use the same primitive hydrostatic system of virtual temperature, humidity, surface pressure and mass continuity prognostic equations on terrain-following sigma (sigma is defined as the ratio of the ambient pressure to surface pressure) coordinates as the GSM used for the NCEP/NCAR Reanalysis.

[10] Except for the scale-dependence built into the horizontal diffusion and some other physical parameterizations, the GSM and RSM physical parameterizations should be, in principle, identical. However, it should be noted that the RSM resembles more the GSM used for the subsequent NCEP/DOE Reanalysis [see *Kanamitsu et al.*, 2002]. The solar radiation parameterization by *Chou and Lee* [1996] replaced the former solar radiation parameterization; however the same *Schwarzkopf and Fels* [1991] long-wave parameterization is still used. As modified by *Hong and Pan* [1996], the GSM/RSM physical package now allows convection to occur when the convective available potential energy (CAPE) is large. There are some other important differences in the boundary layer. In the NCEP/NCAR boundary layer, vertical transfer is related to eddy diffusion coefficients dependent upon a Richardson number-dependent diffusion process [*Kanamitsu*, 1989]. In the current RSM and NCEP/DOE, a non-local diffusion coefficient is used for the mixed layer (diffusion coefficients are still applied above the boundary layer); however turbulent diffusion coefficients are calculated [*Hong and Pan*, 1996] from a prescribed profile shape as a function of boundary layer height and scale parameters derived from similarity requirements [*Troen and Mahrt*, 1986].

[11] In the absence of any regional forcing, (and intrinsic internal dynamics, any significant physical parameterization differences, and significant spatial resolution) the total RSM solution should be identical to the GSM solution. A minor structural difference is that the GSM utilizes vorticity, divergence equations, whereas the RSM utilizes momentum equations in order to have simpler lateral boundary conditions. The GSM and RSM horizontal basis functions are also different. The GSM uses spherical harmonics with a triangular truncation of 62 (T62) whereas the RSM uses cosine or sine waves to represent regional perturbations about the imposed global scale base fields on the regional grids. The double Fourier spectral representations are carefully chosen so that the normal wind perturbations are antisymmetric about the lateral boundary. Other model scalar variables (i.e., virtual temperature, specific humidity, and surface log pressure) are symmetric perturbations. Finally, the RSM usually uses a polar stereographic projection while the GSM uses Gaussian grid, and thus the geographical location of the grids do not match, requiring some interpolation from each grid.

[12] Initial runs with the RSM showed that there was a runaway coupled land-atmosphere feedback that dried out the South American land surface and adversely affected the simulation. This feedback was similar to what had previously occurred in the initial NCEP/NCAR and NCEP/DOE reanalysis runs. In this study we chose to specify the model soil moisture with the daily value from NCEP/NCAR reanalysis. Alternative and better methods were also attempted (see S.-C. Chen and J. Roads, Regional spectral model simulations for South America, manuscript submitted to *Journal of Hydrometeorology*, 2003). Anyway, this empirical fix to the analysis soil moisture was made only for the lower soil moisture level. The upper soil moisture level was left unchanged, since it was felt desirable to have full high-resolution land surface feedback. Other surface prognostic variables, such as ground temperature and canopy water content were initialized once at the beginning of the run and were then left to interact with overlaying atmosphere.

2.2. Florida State Nested Regional Spectral Model (FSUNRSM)

[13] The FSU Nested Regional Spectral Model (FSUNRSM) [*Cocke and LaRow*, 2000] is a similar regional, spectral model. The FSUNRSM also includes a number of user-selectable parameterizations, including 3 radiation schemes and 6 deep convection schemes. For the intercomparison run, FSUNRSM was run with 27 vertically staggered sigma levels, where the moisture (specific humidity) and virtual temperature levels are intermediate to the momentum levels. The physical parameterizations used include the NCAR CCM 3.6 radiation [*Kiehl et al.*, 1998a, 1998b] and the Zhang-McFarlane deep convection [*Zhang and McFarlane*, 1995] scheme. While the BATS and SSiB land surface schemes are currently being implemented, a simplified land surface scheme, which had 24 land use (vegetation) categories (based on USGS data) and 3 soil temperature layers was used here. Soil moisture and albedo are based on vegetation type and season. Planetary boundary layer diffusion is based on *Holtslag and Boville* [1993].

[14] FSUNRSM was designed to be compatible with the FSU Global Spectral Model (FSUGSM), and shares the same vertical structure, dynamics and selection of physical parameterizations. The FSUGSM uses a Gaussian transform grid whereas the FSUNRSM uses a Mercator grid. When the FSUNRSM is nested within the FSUGSM, the base fields and their derivatives from the global model are obtained by a fast Fourier-Legendre transformation directly to the regional grid. When the regional model is nested within reanalysis, as in this study, or within another regional nest, the base fields are bilinearly interpolated to the Mercator grid and the derivatives of the base fields are obtained by finite difference.

2.3. GISS Regional Climate Model

[15] The RCM at GISS/CCSR uses a Cartesian grid with 50-km spacing for dynamics and incorporates interactive soil moisture. The RCM has been used for climate studies over Africa [*Druyan et al.*, 2000, 2001; *Fulakeza et al.*, 2002] and over Brazil [*Druyan et al.*, 2002]. It solves the primitive equations on 16 sigma surfaces using a semi-Lagrangian advection scheme and semi-implicit time differencing with a time step of 465 s. The treatment of

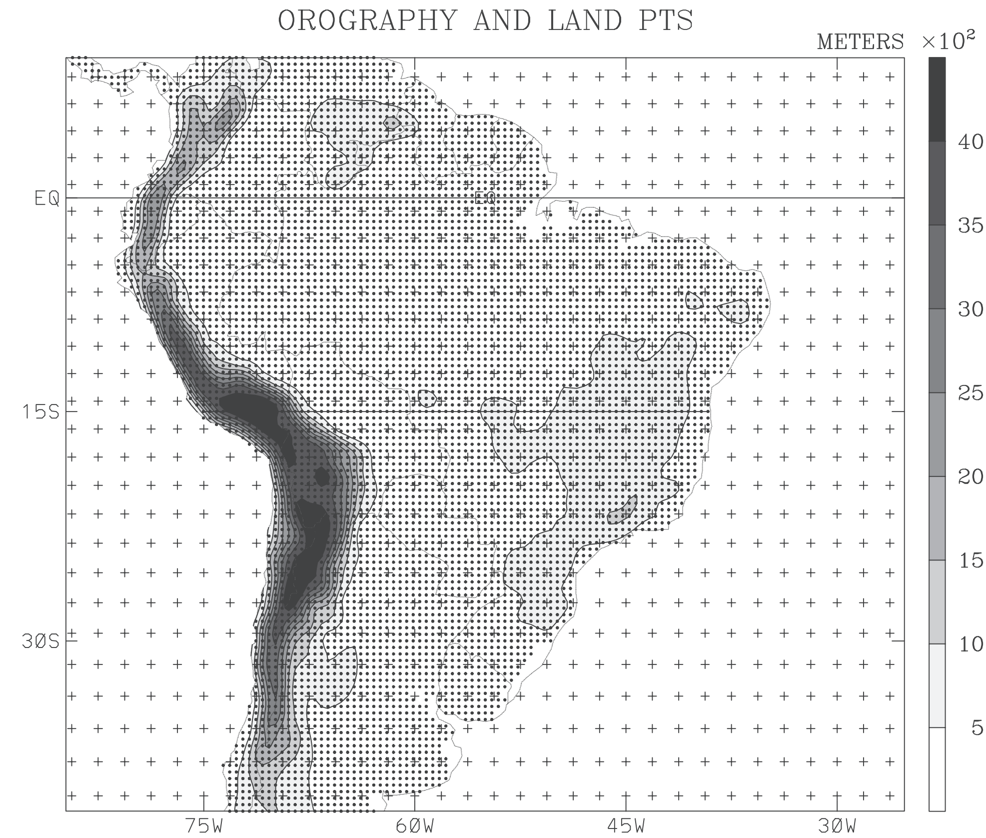

Figure 1. The comparison domain. 85W–25W, 40S–10N, Mercator projection centered at 15S 55W with 50 km resolution. The orography contour interval is 500 meters. Crosses denote the reanalysis grid points, and dots represent the regional model grid points. The line at 15 S denotes the boundary between Northern South America and Southern South America. These areas were sometimes averaged separately.

terrestrial and solar radiation transfer includes diurnal and seasonal variations, absorption by greenhouse gases and interactive clouds. Terrain topography is specified at 0.5° resolution, consistent with the horizontal computing grid. Deep convection is parameterized by the Kuo scheme, modified according to *Krishnamurti et al.* [1990].

[16] Soil moisture availability (SMA) is defined as the ratio of soil moisture at the surface to a maximum field capacity. The scheme, which updates SMA, was derived by computing a range of values based on estimates of evaporation (latent heat flux) derived from moisture continuity considerations and estimates of the surface radiative energy balance. These SMA values were subsequently used as the dependent variable in second-order regression against observed 5-day rainfall, albedo, surface temperature, normalized difference vegetation index (NDVI) and terrain relief, from data for southern Africa. The derived second-order regression equation constitutes the RCM's interactive scheme, which determines SMA during model simulations. *Fulakeza et al.* [2002] demonstrate how the regression can be made separately for each of several soil types in order to increase its sensitivity to local ground conditions, although in the present study a single function is used for all land grid elements using multiyear mean values of NDVI. The evolution of modeled surface albedo depends solely on the computed SMA. In summary, the RCM computes SMA interactively as a function of model rainfall, albedo and surface temperature and NDVI. The scheme does not require a long spin-up to charge the groundwater reservoir, but rather creates evolving SMA distributions early in the simulations that remain fully compatible with the model's local precipitation and temperature history. *Fulakeza et al.* [2002] showed that RCM-predicted soil moisture and albedo have an impact on simulated rainfall over southern Africa through the modification of sensible and latent heat fluxes.

[17] Prescribed lateral boundary conditions force the predicted RCM evolution by weighting them with progressively decreasing weights inward within a six-grid buffer zone that completely surrounds the domain of interest.

2.4. IRI Regional Climate Model

[18] Although the IRI is using the same regional model as the Scripps ECPC (described above), the regional climate model used for this comparison was RegCM2, developed by *Giorgi et al.* [1993a, 1993b]. This model has been used extensively for regional climate studies over the regions such as the United States [*Mearns et al.*, 2001], Europe [*Giorgi and Marinucci*, 1996], East Asia [*Liu et al.*, 1994], Africa [*Indeje et al.*, 2001], and South America (J.-H. Qian, A. Seth, and S. Zebiak, Reinitialized versus continuous simulations for regional climate downscaling, manuscript submitted to *Monthly Weather Review*, 2002). A regional variable resolution scheme was also developed for the model [*Qian et al.*, 1999]. The dynamical core of RegCM2 is essentially that of the Penn State/NCAR Mesoscale

Model version 4.0 (MM4), a grid point model (with Arakawa-B grid) based on hydrostatic, compressible atmospheric equations. The vertical resolution is based on a pressure-based terrain-following coordinate. The regional model can be driven by lateral boundary conditions provided by either reanalysis or GCM prediction. To avoid discrepancies between the outer driving fields and the model internal physics, an exponential relaxation scheme is applied at the lateral buffer-zone with a width of 14 grid intervals, a weighted averaging between the driving field and the model simulated field with the weight for the former being 1 at the outer boundary and exponentially diminishing to 0 at the inner boundary of the buffer-zone.

[19] The regional model is totally governed by its own physics in the inner domain surrounded by the lateral buffer zone, only subject to the forcing by the underlying lower boundary of land and ocean. Over land area, the Biosphere Atmosphere Transfer Scheme (BATS) [*Dickinson et al.*, 1993] is employed to compute surface radiative, sensible and latent heat, momentum fluxes, and surface temperature based on the assigned vegetation and soil parameters. While over the ocean, the model is forced by the sea surface temperature (SST) spatially and temporally interpolated from a monthly SST data set. The resolvable scale precipitation is calculated by a simplified explicit moisture scheme described by *Giorgi and Shields* [1999] and the cloud water and fractional cover are used for cloud-radiation computations. The Grell cumulus scheme [*Grell*, 1993] is used to calculate the precipitation due to moist convection. The parameterization scheme of the diabatic heating by solar and terrestrial radiations is that of the NCAR Community Climate Model CCM3 [*Kiehl et al.*, 1998a, 1998b]. The parameterization representing subgrid-scale processes in the planetary boundary layer, such as turbulent transfer of momentum and heat in the lower atmosphere, is that of *Holtslag et al.* [1990].

[20] For this domain, the model was run with a uniform grid of 50 km on a Mercator projection map. The model has 14 vertical levels with 5 levels in the lowest 1.5 km of the atmosphere and the top of the model atmosphere is at 80 hPa. The model was run from Feb 21, 1997 to April 10, 1999, with a time step of 1.5 min.

2.5. Observations

[21] *Xie and Arkin* [1997] developed a monthly mean global precipitation data set at 2.5° resolution that not only extends back to 1979 but also provides higher temporal resolution (pentads) over land and ocean. In response to a number of requests, an experimental land only precipitation data set from gauges only was subsequently developed at daily timescales and 0.5° resolution. This data set is highly correlated with the standard monthly mean product and was chosen here as the optimal data set for comparing these higher resolution models. We shall refer to this data as observations henceforth.

3. Experiment Methodology

3.1. Experiment Design

[22] All regional model simulations were forced by large-scale boundary conditions from the NCEP/NCAR reanalysis I [*Kalnay et al.*, 1996]. NCEP/NCAR reanalysis I forcing variables included surface pressure, atmospheric virtual temperature and relative humidity, and atmospheric winds. In particular, all model variables were nudged at the lateral boundary (the RSM and FSUNRSM also needed the interior large-scale analyses to develop interior perturbations that could be filtered) with updated reanalysis 4× daily. Several auxiliary fields from the reanalysis, including: sea surface temperatures, soil moisture, vegetation, high-resolution orography, were also used by the participants. It should be noted that the original reanalysis global spectral data was actually converted to a grid point area, which covers an area (not shown) somewhat larger than the evaluation domain. The ECPC has found that this conversion of the global spectral data to limited area regional grid point data is the most efficient way to transfer global forecast and analysis data needed for regional models.

[23] Following an initialization at the beginning of the period, all of the simulations were run and archived continuously (daily) from for the period 1 March 1997 through 30 April 1999. During this period, one of the strongest El Nino's of all time occurred during the southern hemisphere summer of 1997/1998, which was then followed by a strong La Nina pattern the following summer (1998/1999).

[24] Figure 1 shows the comparison domain. Again, the actual model domains are only slightly larger than shown here (about 3 grid points), and somewhat different from model to model depending on the individual model need for the lateral boundary nudging area size. All regional models

Table 2. Area Mean, Systematic Error, Standard Deviation, Correlation, Normalized Covariance, Standard Deviation of Normalized Covariance Time Series[a]

	Mean	SE	Std.	Corr.	Norm. Cov.	Std. Cov.
			Southern South America			
Xie0.5	2.69		2.09			
Xie2.5	2.88	0.19	1.85	0.82	0.86	0.07
Reanalysis	3.15	0.46	2.14	0.62	0.55	0.21
RSM	2.67	−0.02	2.59	0.47	0.46	0.21
FSUNRSM	3.47	0.78	1.98	0.38	0.29	0.22
RegCM2	3.16	0.47	2.54	0.50	0.52	0.23
RCM	3.09	0.4	2.52	0.14	0.13	0.32
Ensemble	3.10	0.41	1.78	0.49	0.45	0.26
			Northern South America			
Xie0.5	4.07		2.80			
Xie2.5	4.14	0.07	2.30	0.84	0.81	0.08
Reanalysis	5.62	1.55	2.34	0.45	0.38	0.24
RSM	3.92	−0.15	2.54	0.34	0.32	0.21
FSUNRSM	4.00	−0.07	1.69	0.14	0.13	0.21
RegCM2	3.23	−0.84	2.90	0.34	0.33	0.20
RCM	5.28	1.21	3.36	0.29	0.25	0.24
Ensemble	4.11	0.04	1.81	0.41	0.39	0.21
			South America			
Xie0.5	3.47		2.51			
Xie2.5	3.59	0.12	2.11	0.83	0.83	0.06
Reanalysis	4.53	1.06	2.26	0.53	0.44	0.19
RSM	3.37	−0.1	2.56	0.40	0.38	0.16
FSUNRSM	3.77	0.3	1.82	0.25	0.19	0.17
RegCM2	3.20	−0.27	2.74	0.41	0.40	0.17
RCM	4.31	0.84	3.02	0.22	0.22	0.20
Ensemble	3.66	0.19	1.79	0.45	0.42	0.17

[a]Area mean (Mean, mm/day), systematic error (SE, mm/day), standard deviation (Std., mm/day), Correlation (Corr.), Normalized Covariance (Cov.), standard deviation of normalized covariance time series (Std. Cov.).

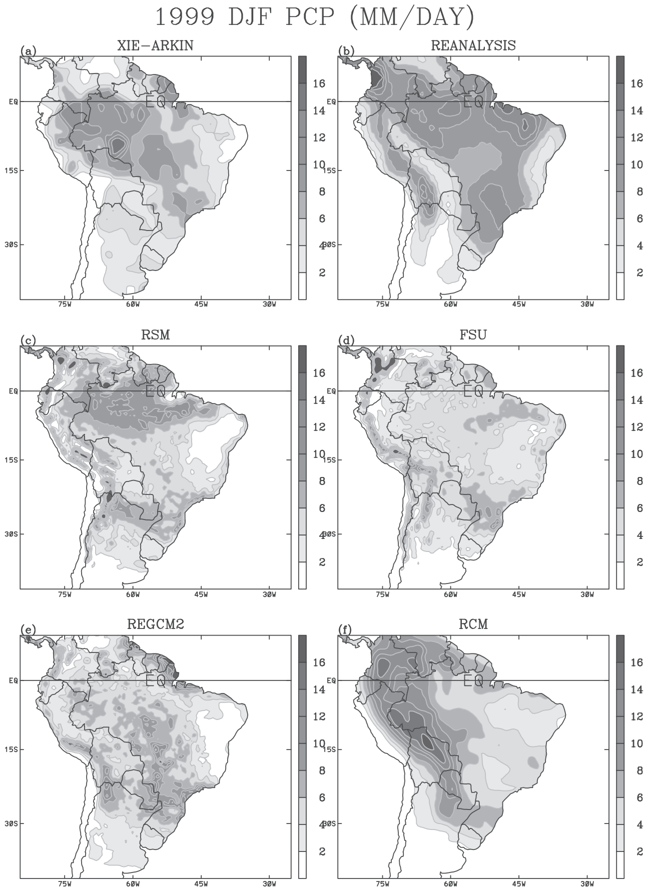

Figure 2. 1998/1999 DJF precipitation (mm/day) from (a) Xie-Arkin observations, (b) Reanalysis, (c) RSM, (d) FSUNRSM, (e) RegCM2, and (f) RCM.

were run at 50 km horizontal resolution but varying vertical resolution. The grid points indicate the land regions (separated to northern and southern regions at 15S), where the comparison was made for area averages. The northern and southern land regions are hereafter denoted in this paper as Northern South America, Southern South America, and the entire domain is denoted South America.

3.2. Skill Measures

[25] Skill is measured in a number of different ways. We are first of all interested in the mean climatology.

$$\bar{A} = \sum A$$

where the sum is over the appropriate time period. For example, we sum individual months separately so we can develop a monthly climatology. The average difference between the models (A) and observations (B) is referred to as a bias and all imperfect models will have a bias

$$\bar{A} - \bar{B} = \sum (A - B)$$

which is one measure of the model skill.

[26] We are also interested in the monthly anomalies from these monthly climatologies. That is,

$$A' = A - \bar{A}$$

These anomalies will have a statistical distribution that can be characterized by the standard deviation

$$SD = \left(\frac{1}{N-1}\sum A'^2\right)^{1/2}$$

The average skill in depicting the overall variability can be measured by the correlation

$$CORR2 = \frac{\sum A'B' - \sum A' \sum B'}{\left(\left(\sum A'^2 - \left(\sum A'\right)^2\right)\left(\sum B'^2 - \left(\sum B'\right)^2\right)\right)^{1/2}}$$

where the summation is over time and space (weighted by the cosine of latitude). A spatial correlation can also be computed for each time period and the time average of this correlation (CORR1) is always less than CORR2 since times when the entire area are anomalously high or low tend to have low correlation. In fact, *Roads et al.* [2001] suggested that the time average of the normalized covariance (ACOV) was more representative of the overall correlation than the time averages of individual correlations. In any event, both correlations provide a measure of the overall skill. There is one additional parameter that is of interest, which is the standard deviation of the normalized

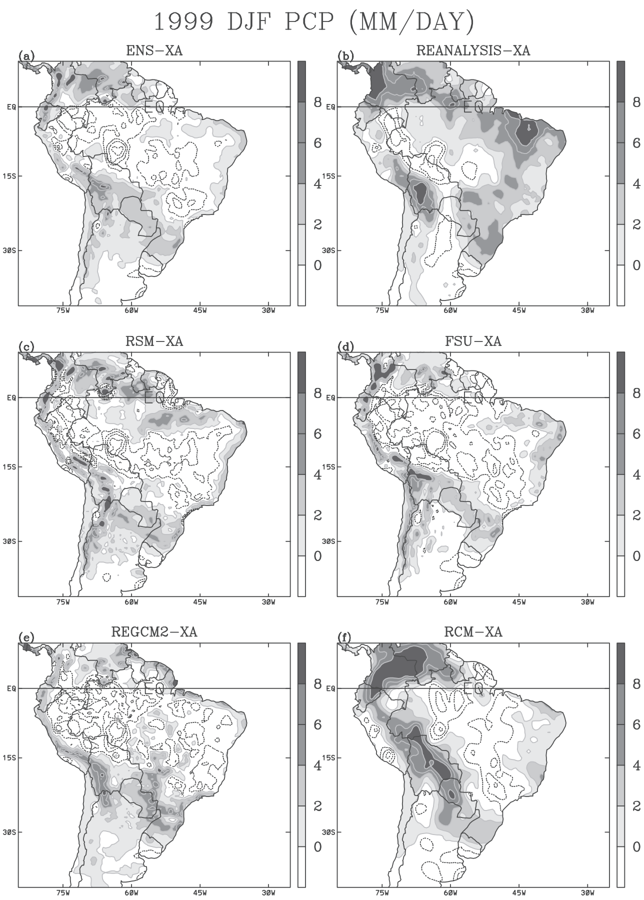

Figure 3. 1998/1999 DJF precipitation systematic errors (mm/day) from (a) regional model ensemble mean, (b) Reanalysis, (c) RSM, (d) FSUNRSM, (e) RegCM2, and (f) RCM.

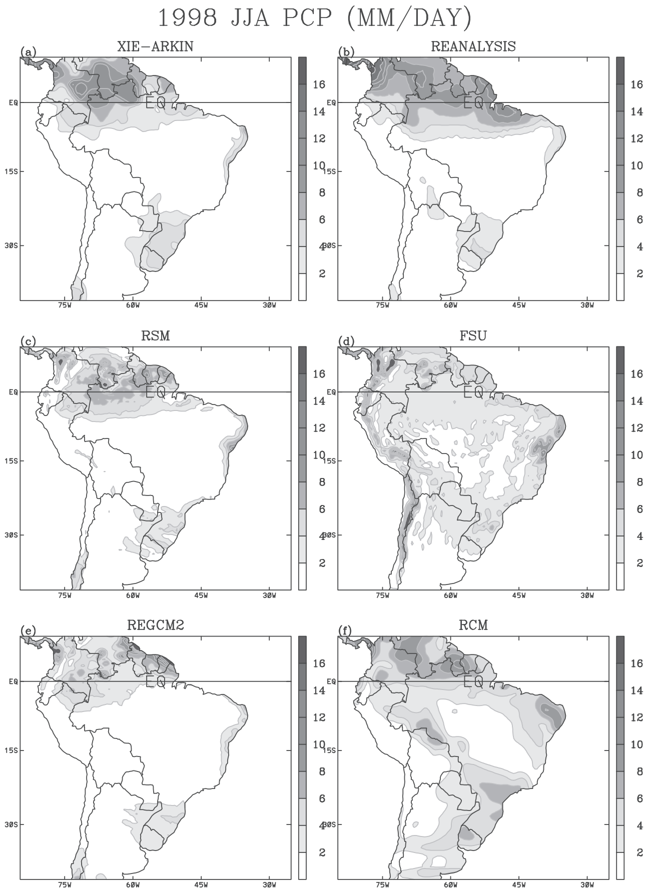

Figure 4. 1998 JJA precipitation (mm/day) from (a) Xie-Arkin observations, (b) Reanalysis, (c) RSM, (d) FSUNRSM, (e) RegCM2, and (f) RCM.

covariance time series. Dividing this value by the square root of the number of independent observations provides some measure of the significance of the time-averaged correlations. For example Table 2 indicates that for these normalized covariance time series the standard deviation is about 0.25 and dividing by square root of 24 independent events indicates a standard deviation of about 0.05. More than two standard deviations are required at the 95% level and hence correlations must be greater than0.1 to be significantly different from each other and zero.

[27] NCEP threat and bias scores are used here to further assess the precipitation skill for more intense precipitation [see *Mesinger and Black*, 1992]. The equitable threat score is defined as

$$ET = \frac{H - CH}{F + O - H - CH}$$

where F and O are the number of forecast and observation points in the evaluation domain that have precipitation above a certain threshold. H is the grid point number of correct forecast ("hit") above a threshold. CH is the expected number of hits in a random forecast of F and observed O and has the form

$$CH = \frac{F \times O}{N}$$

where N is the total number of points over the evaluation domain. Basically, the threat score is scaled so that zero indicates random predictions and 1 indicates perfect forecasts.

[28] The bias score is the ratio of the forecast and observed points and is defined as

$$BIAS = \frac{F}{O}$$

A bias value above (below) 1 indicates a model wet (dry) bias. To weight the different geographic errors, we sum the cosine of the latitude associated with each grid point.

4. Results

[29] Figure 2 shows the December, January, February (DJF) 1998/1999 precipitation simulation by the 4 regional models in comparison to the precipitation from the driving reanalysis and observations. This period corresponds to the seasonally wet and warm period when the South American Monsoon precipitation is more active over the land, especially on the eastern and northern edge of the Amazon basin where the tropical trade winds are blocked by the Andes.

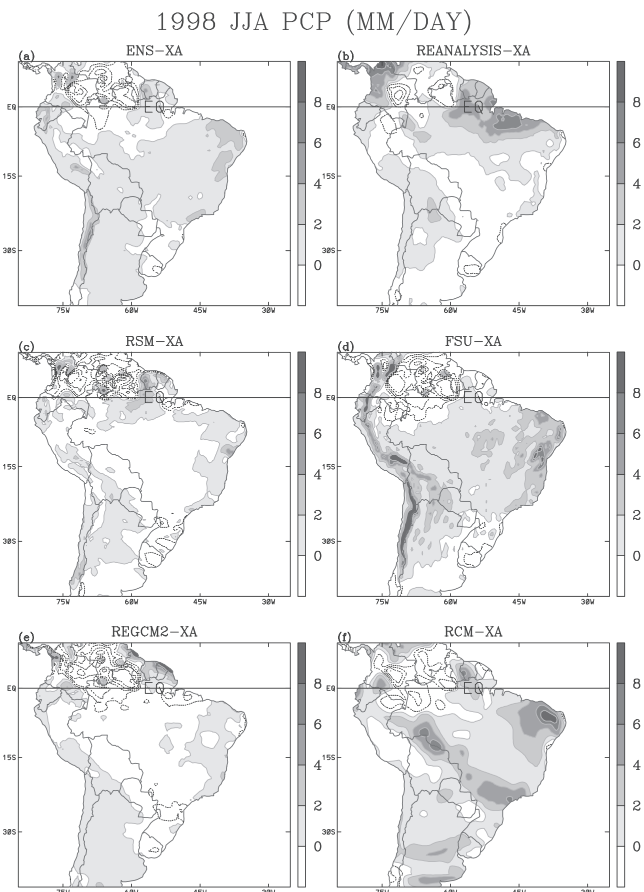

Figure 5. 1998 JJA precipitation systematic errors (mm/day) from (a) regional model ensemble mean, (b) Reanalysis, (c) RSM, (d) FSUNRSM, (e) RegCM2, and (f) RCM.

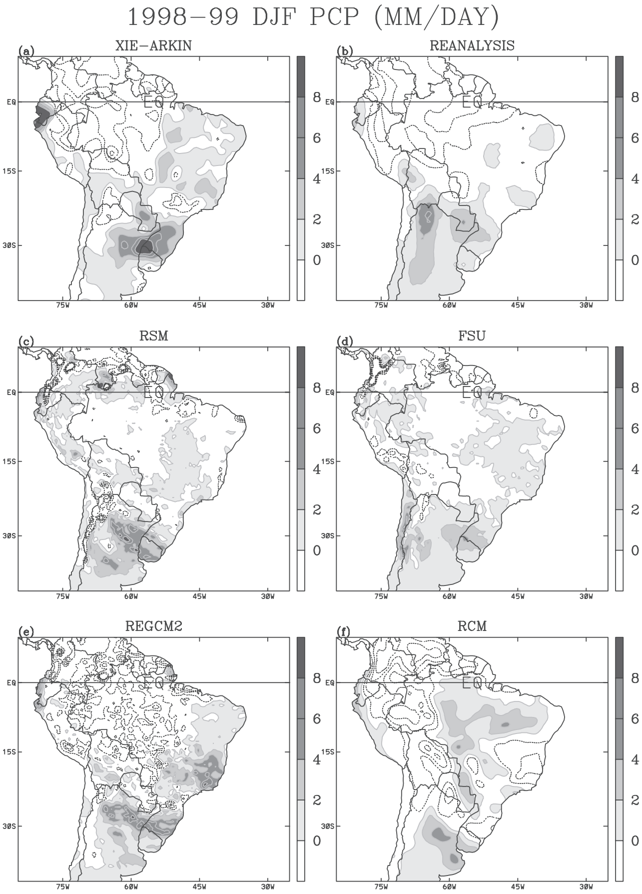

Figure 6. 1997/1998 minus 1998/1999 DJF interannual precipitation variations (mm/day) from (a) Xie-Arkin observations, (b) Reanalysis, (c) RSM, (d) FSUNRSM, (e) RegCM2, and (f) RCM.

This period also occurred during a La Nina episode, when northern Brazil is expected to be anomalously wet. The reanalysis and all models reflect the observed maxima of the summer monsoon, although the reanalysis is overly wet over most of eastern Brazil. Despite this bias of the regime forcing the limited area model simulations, the regional models appear to be overly dry over much of Brazil, which is shown more clearly by looking at the systematic error (model - XA) in Figure 3. Underestimates of seasonal precipitation rates do not occur in the same regions for all models so errors are somewhat muted in the ensemble mean, indicating one advantage of a multimodel ensemble. This is shown most clearly in Table 2, where the ensemble mean systematic error is close to the lowest error of all the models.

[30] Figure 4 shows the JJA 1998 precipitation simulation by the 4 regional models in comparison to the precipitation from the driving reanalysis and observations. This period corresponds to the seasonally dry and cool period when the precipitation is more active over the surrounding ocean. The reanalysis and all models simulate the main features of the observations although the FSUNRSM and RCM tend to have too much Southern Hemisphere precipitation while the RegCM2 underestimates rainfall over the eastern portions of the Amazon. However, it is clear that the regional models have at least captured the seasonal cycle and can distinguish between the seasonal wet and dry period. Again, as shown in Figure 5, the ensemble model mean appears to have the smallest errors although all models, and the ensemble mean, tend to have too little precipitation in the northeast, which may be related in part to the commonality of the reanalysis data which forced these simulations.

[31] Figure 6 shows the interannual differences between the 1997/1998 and 1998/1999 DJF precipitation. Again, during this period one of the strongest El Nino, La Nina cycles occurred, resulting in increased dryness over much of Brazil during 1997/1998 and increased precipitation to the south over the La Plata during the early part of the period. The reanalysis provides a qualitatively correct depiction of the interannual precipitation variations, which is then emulated, more or less, by all the models. However, it is clear that there are a number of systematic errors and the ensemble mean (Figure 7) again appears to have the smallest error. In particular, all models underestimated the opposite, rather extreme observed interannual differences over the Equatorial northwest and over the La Plata Basin. Also noticeable are the distinct small-scale features of the RegCM2, FSUNRSM, and RSM models, which do not

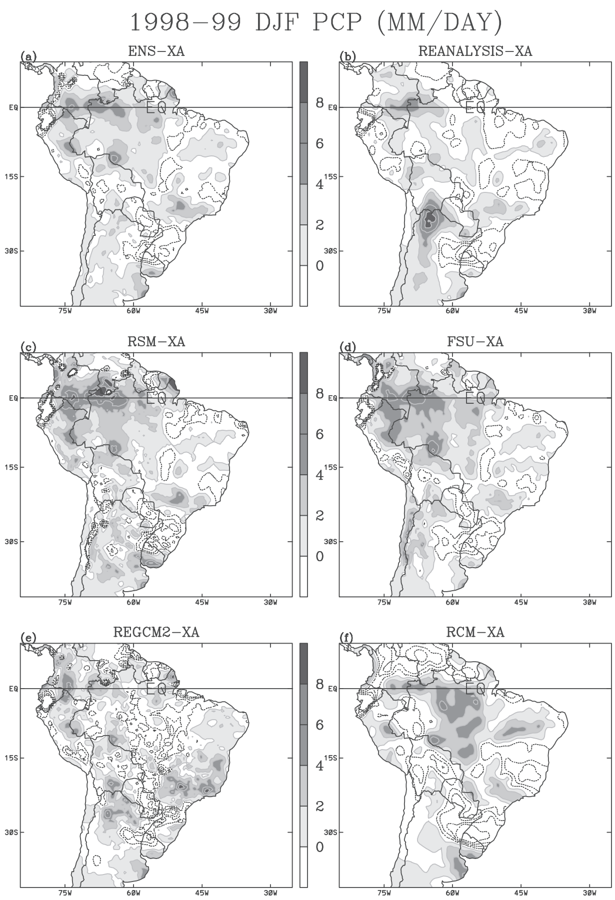

Figure 7. 1997/1998 minus 1998/1999 DJF interannual precipitation variations systematic errors (mm/day) from (a) regional model ensemble mean, (b) Reanalysis, (c) RSM, (d) FSUNRSM, (e) RegCM2, and (f) RCM.

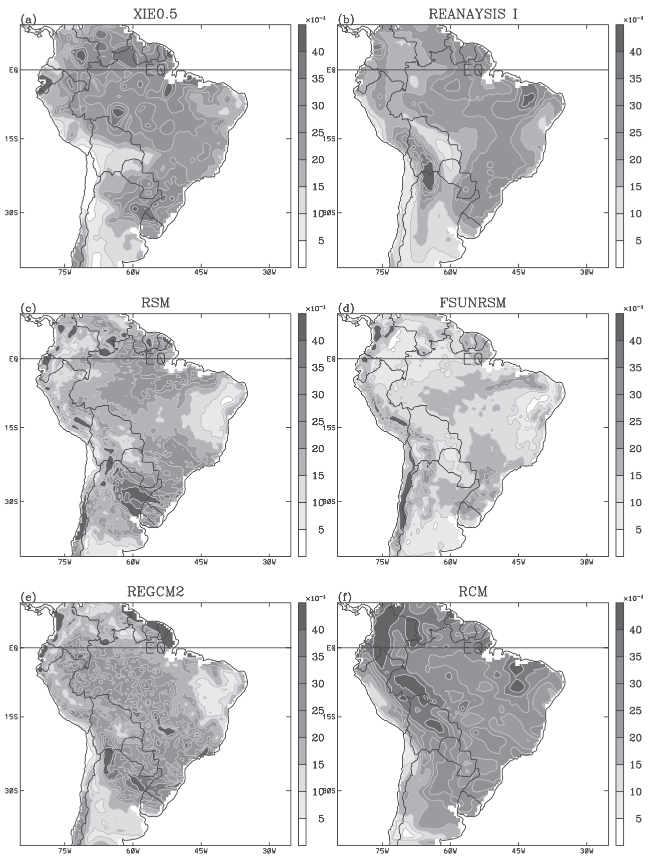

Figure 8. Standard deviation (mm/day) for (a) Xie-Arkin observations, (b) Reanalysis, (c) RSM, (d) FSUNRSM, (e) RegCM2, and (f) RCM.

appear in the reanalysis or the *Xie and Arkin* [1997] 0.5° analysis.

[32] Figure 8 shows the temporal standard deviations for the time series of daily precipitation rates, March 1997–April 1999 for observations and models. Area mean values are provided in Table 2. SD for the reanalysis and RSM are only somewhat lower than the observed values. By contrast the RegCM2 and especially the RCM tend to have excessive variability. The FSUNRSM had too little variability, except over the Andes, where the SD was excessive. In fact all models, including the reanalysis had too much variability in the vicinity of the Andes, suggesting problems near steep topography.

[33] Figure 9 displays the correlations between simulated daily precipitation rates versus observations for each model and for the ensemble mean. Clearly the reanalysis is quite useful for describing the precipitation over South America, the major exceptions being northern Peru and Colombia, Bolivian Antiplano, and Northeast Brazil. The ensemble regional model mean increases this correlation somewhat over Bolivia and central Brazil and the La Plata but Peru is still problematic, perhaps in part because it lies on the lee side of the Andes and windward sides tend to be more predictable. Similar features occur in the other models, and again after the reanalysis the ensemble mean had the greatest overall correlation (Table 2). All models tend to have stronger correlations over Argentina than over Brazil, which appears to be most problematic for the regional models. Presumably this is due in part to the lack of orography to guide the models, and perhaps partly due to inadequate land surface parameterizations. For example, the somewhat better correlated model, the RSM, presumably benefits from the corrected lower level soil moisture. Again, previous experiments showed that without this correction, the model becomes overly dry causing a major impact on the simulation.

[34] Figure 10 shows the time series for the basin means (Figure 10a) of the models and the *Xie and Arkin* [1997] precipitation observations for South America. The reanalysis has an overall positive systematic error in the area mean (Figure 10b), which again is reduced by the ensemble average. Although the curves are not labeled, further examination indicates that the RCM results incur the largest deviations from the ensemble average in both the area means and standard deviations (Figure 10c). The reduced spatial standard deviation is one of the drawbacks of using ensembles to characterize natural behavior. Finally, the normalized covariance (Figure 10d), demonstrates that the ensemble mean and reanalysis usually have the highest normalized covariance and (Table 2) the highest correlation. RSM and RegCM2 correlations are also fairly high. There does appear to be skill during summer and winter with the transition seasons (spring and fall) being the least skillful. This may be typical of tropical regimes.

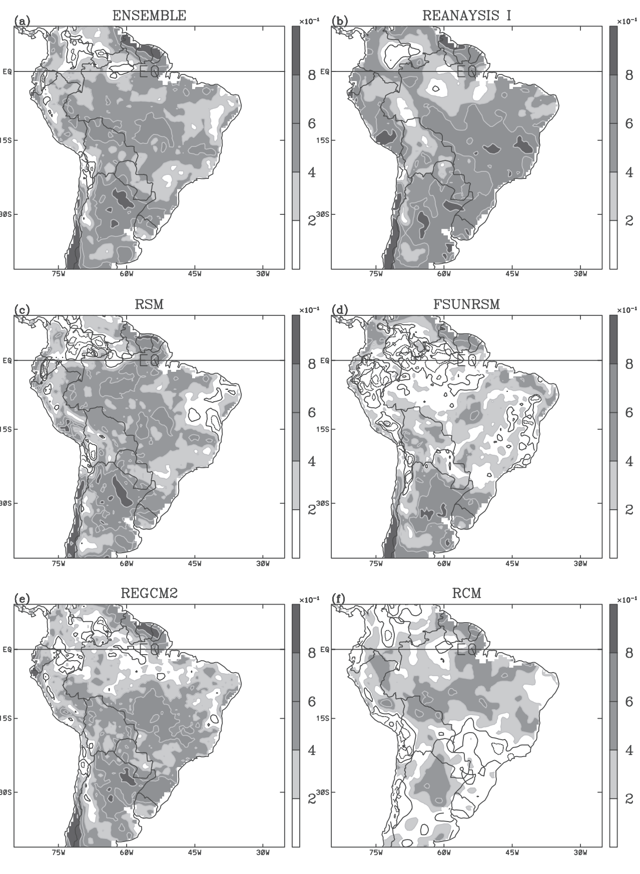

Figure 9. Correlations between observations and (a) regional model ensemble mean, (b) Reanalysis, (c) RSM, (d) FSUNRSM, (e) RegCM2, and (f) RCM.

[35] Figure 11a shows the NCEP and model threat scores for monthly mean precipitation. The highest threat scores were achieved by the RSM, the reanalysis and the ensemble mean. The RegCM2 and the RCM had only slightly lower threat scores for mid-range precipitation thresholds. *Roads et al.* [2003] has shown that the threat scores for lower precipitation intensities can be improved simply by making one-day forecasts starting from the analysis. Doing this would presumably achieve monotonically increasing scores with decreasing threshold. In that regard, note that the skill of all systems deteriorates rapidly for thresholds exceeding 5 mm day^{-1}. The decrease in skill at high thresholds for the ensemble mean is a result of smoothing, suggesting that the effects of ensemble smoothing may need to be taken into account when simulating extreme events.

[36] The reanalysis bias Figure 11b is somewhat decreased by the various regional models and ensemble mean. Whereas the reanalysis bias is large for moderate thresholds (5–15 mm day^{-1}), the ensemble mean bias is quite low (good) in this range. Unfortunately, while most of the regional models show neutral bias below 4 mm day^{-1}, they all suffer from large exaggerations of the largest monthly mean rates. This may be related to the overly intense precipitation on the tops of mountains shown in Figures 2–7. In the RSM preliminary experiments have indicated this may be due to an unrealistic representation of moisture diffusion, although more extensive tests are still needed.

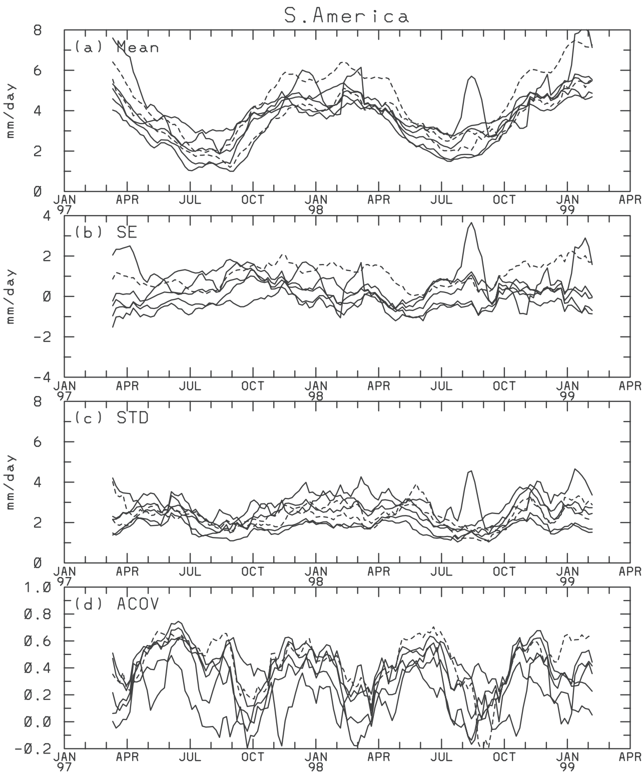

Figure 10. South America monthly mean time series (March 1997–Feburary 1999) for observations (thin dashed line), reanalysis (thick dashed line), ensemble mean (thick solid line) and individual models (thin solid lines) for the total land area: (a) area means, mm/day; (b) systematic error, SE, mm/day; (c) standard deviation, STD, mm/day; (d) normalized covariance, ACOV.

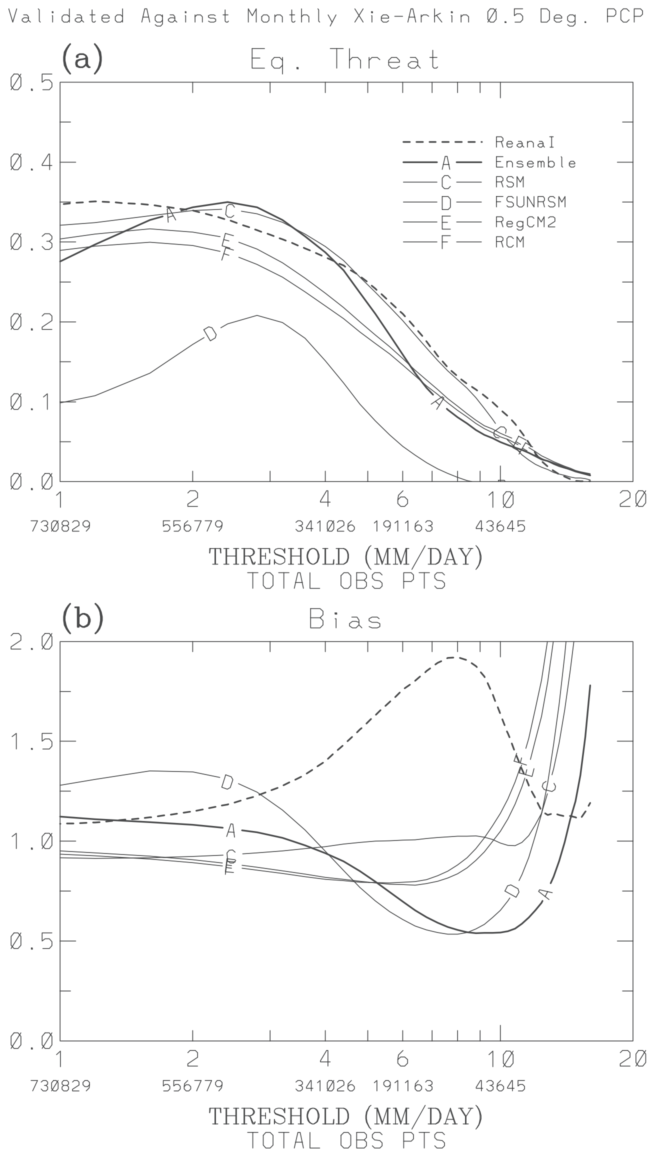

Figure 11. South America precipitation equitable threat and bias skill scores for NCEP/NCAR Reanalysis (dashed line), regional model ensemble mean (A), RSM (C), FSUNRSM (D), RegCM2 (E), RCM (F): (a) equitable threat; (b) bias.

5. Summary

[37] A community regional modeling intercomparison project among the: (1) Scripps Experimental Climate Prediction Center regional spectral model (RSM), (2) Florida State Univ. nested regional spectral model (FSUNRSM), (3) Goddard Institute for Space Studies regional climate model (RCM), and (4) IRI regional climate model (RegCM2) for South America was described. In comparison to observations, the regional models had systematic precipitation errors that were somewhat similar to the driving NCEP/NCAR reanalysis systematic error, although at least the regional model ensemble mean errors were somewhat

smaller. However, the ensemble mean area standard deviations were somewhat less than for individual models and the observations, indicating that averaging individual model runs resulted in reduced spatial variance without necessarily providing the smallest RMS errors. Threat and bias scores indicated that the reanalysis and the ensemble mean of all the models provided the best skill.

[38] This intercomparison showed that it is now feasible to begin to make regional model simulations embedded within the reanalysis with a variety of models. The results were encouraging in that the ensemble mean of the regional simulations sometimes provided a somewhat better simulation of the precipitation than was present in the original reanalysis. However, all models had similar noticable large-scale biases, which seem to be influenced by the forcing large-scale reanalysis, which could have partially biased the ensemble mean. It might be better, for example, to use multiple large-scale analyses forcing multiple regional models to develop the best overall climate description.

[39] Unfortunately, it is clear that regional models, despite all their promise, still do not noticeably improve upon the large-scale driving analyses. We suspect that one reason for this lack of improvement is that most regional scale parameterizations have really been derived for coarser-scale general circulation models and these low-resolution parameterizations have not been optimally tuned for regional models. As discussed by *Roads et al.* [2003] and *Han and Roads* [2003], it may therefore be best for the time being to defocus on obtaining high-resolution simulations so that larger coarse-scale regional ensembles can be developed. Again, regional models are certainly useful for taking advantage of regional data sets and emphasizing particular regional domains.

[40] **Acknowledgments.** ECPC research was funded by a cooperative agreement from NOAA-NA17RJ1231 and USDA FS 01-CA-11272169-149 and NASA NAG8-1875. Work at the Earth Institute at Columbia University was supported by an intramural grant from the International Research Institute for Climate Research and NSF Grant ATM 00-89563. The views expressed herein are those of the authors and do not necessarily reflect the views of NOAA, USDA, NSF and NASA.

References

Anderson, B. T., J. O. Roads, S.-C. Chen, and H.-M. H. Juang, Regional simulation of the low-level monsoon winds over the Gulf of California and southwest United States, *J. Geophys. Res.*, *105*, 17,955–17,969, 2000a.

Aderson, B. T., J. O. Roads, and S.-C. Chen, Large-scale forcing of summertime monsoon surges over the Gulf of California and southwest United States, *J. Geophys. Res.*, *105*, 455–467, 2000b.

Anderson, B. T., J. O. Roads, S.-C. Chen, and H.-M. H. Juang, Model dynamics of summertime low-level jets over Northwest Mexico, *J. Geophys. Res.*, *106*, 3401–3413, 2001.

Anthes, R. A., Y. H. Kuo, E. Y. Hsie, S. Low-Nam, and T. W. Bettge, Estimation of episodic and climatological skill and uncertainty in regional numerical models, *Q. J. R. Meteorol. Soc.*, *115*, 763–806, 1989.

Chen, S.-C., J. O. Roads, H.-M. H. Juang, and M. Kanamitsu, Global to regional simulation of California wintertime precipitation, *J. Geophys. Res.*, *104*, 31,517–31,532, 1999.

Chen, S.-C., M.-C. Wu, S. Marshall, H.-M. Juang, and J. O. Roads, $2\times CO_2$ Eastern Asia regional responses in the RSM/CCM3 modeling system, *Global Planet. Change*, *37*, 277–285, 2003.

Chou, M.-D., and K.-T. Lee, Parameterizations for the absorption of solar radiation by water vapor and ozone, *J. Atmos. Sci.*, *53*, 1203–1208, 1996.

Cocke, S., and T. E. LaRow, Seasonal predictions using a regional spectral model embedded within a coupled ocean-atmosphere model, *Mon. Weather Rev.*, *128*, 689–708, 2000.

Dickinson, R. E., R. M. Errico, F. Giorgi, and G. T. Bates, A regional climate model for the western United States, *Clim. Change*, *15*, 383–422, 1989.

Dickinson, R. E., A. Henderson-Sellers, and P. J. Kennedy, Biosphere atmosphere transfer scheme (BATS) version 1e as coupled to the NCAR community climate model, NCAR Technical Note, *NCAR/TN-387 + STR*, 72 pp., Natl. Cent. for Atmos. Res., Boulder, Colo., 1993.

DiMego, G. J., K. E. Mitchell, R. A. Petersen, J. E. Hoke, J. P. Gerrity, J. J. Tuccillo, R. L. Wobus, and H.-M. H. Juang, Changes to NMC's regional analysis and forecast system, *Weather Forecasting*, *7*, 185–198, 1992.

Druyan, L., M. Fulakeza, and W. Thiaw, Regional model simulations of African wave disturbances, *J. Geophys. Res.*, *105*, 7231–7255, 2000.

Druyan, L., M. Fulakeza, P. Lonergan, and M. Saloum, A regional model study of synoptic features over West Africa, *Mon. Weather Rev.*, *129*, 1564–1577, 2001.

Druyan, L., M. Fulakeza, and P. Lonergan, Dynamic downscaling of seasonal climate predictions over Brazil, *J. Clim.*, *15*, 3411–3426, 2002.

Fulakeza, M., L. Druyan, and T. Krishnamurti, A simple soil moisture scheme for climate simulations in the tropics, *Meteorol. Atmos. Phys.*, *79*, 105–126, 2002.

Giorgi, F., and G. T. Bates, On the climatological skill of a regional model over complex terrain, *Mon. Weather Rev.*, *117*, 2325–2347, 1989.

Giorgi, F., and M. R. Marinucci, A study of sensitivity of simulated precipitation to model resolution and its implications for climate studies, *Mon. Weather Rev.*, *124*, 148–166, 1996.

Giorgi, F., and C. Shields, Tests of precipitation parameterizations available in the latest version of NCAR regional climate model (RegCM) over continental Unites States, *J. Geophys. Res.*, *104*, 6353–6375, 1999.

Giorgi, F., M. R. Marinucci, and G. T. Bates, Development of a second-generation regional climate model (RegCM2): Part I. Boundary layer and radiative transfer processes, *Mon. Weather Rev.*, *121*, 2794–2813, 1993a.

Giorgi, F., M. R. Marinucci, and G. T. Bates, Development of a second-generation regional climate model (RegCM2): Part II. Convective processes and assimilation of lateral boundary conditions, *Mon. Weather Rev.*, *121*, 2814–2832, 1993b.

Grell, G. A., Prognostic evaluation of assumptions used by cumulus parameterizations, *Mon. Weather Rev.*, *121*, 764–787, 1993.

Han, J., and J. Roads, U.S. climate sensitivity simulated with the NCEP regional spectral model, *J. Clim. Change*, in press, 2003.

Harshvardhan, S., and T. Corsetti, Long wave parameterization for the UCLA/GLAS GCM, *NASA Tech. Memo 86072*, Greenbelt, Md., 1984.

Hastenrath, S., and L. Grieschar, Circulation mechanisms related to northeast Brazil rainfall anomalies, *J. Geophys. Res.*, *98*, 5093–5102, 1993.

Hastenrath, S., and L. Heller, Dynamics of climatic hazards in Northeast Brazil, *Q. J. R. Meteorol. Soc.*, *103*, 411–425, 1977.

Hirakuchi, H., and F. Giorgi, Multi-yr present day and $2 \times CO_2$ simulations of monsoon climate over eastern Asia and Japan with a regional climate model nested in a general circulation model, *J. Geophys. Res.*, *100*, 21,105–21,126, 1995.

Holtslag, A. A. M., and B. A. Boville, Local versus non-local boundary layer diffusion in a global climate model, *J. Clim.*, *6*, 1825–1842, 1993.

Holtslag, A. A. M., E. I. F. de Bruijn, and H.-L. Pan, A high-resolution air mass transformation model for short-range weather forecasting, *Mon. Weather Rev.*, *118*, 1561–1575, 1990.

Hong, S., and A. Leetma, An evaluation of the NCEP RSM for regional climate modeling, *J. Clim.*, *12*, 592–609, 1999.

Hong, S., and H. Pan, Nonlocal boundary layer vertical diffusion in a medium-range-forecast model, *Mon. Weather Rev.*, *124*, 2322–2339, 1996.

Horel, J. D., J. B. Pechman, A. N. Hahman, and J. E. Geisler, Simulation of the Amazon basin circulation with a regional model, *J. Clim.*, *7*, 56–71, 1994.

Indeje, M., F. H. M. Semazzi, L. Xie, and L. J. Ogallo, Mechanistic model simulations of the East African climate using NCAR Regional Climate Model: Influence of large-scale orography on the Turkana low-level jet, *J. Clim.*, *14*, 2710–2724, 2001.

Ji, Y., and A. D. Vernekar, Simulation of the Asian summer monsoons of 1987 and 1988 with a regional spectral model nested in a global GCM, *J. Clim.*, *10*, 1965–1979, 1997.

Jones, R. G., J. M. Murphy, and M. Noguer, Simulation of climate change over Europe using a nested regional climate model: I. Assessment of control climate, including sensitivity to location of lateral boundaries, *Q. J. R. Meteorol. Soc.*, *121*, 1413–1449, 1995.

Juang, H.-M. H., and M. Kanamitsu, The NMC nested regional spectral model, *Mon. Weather Rev.*, *122*, 3–26, 1994.

Juang, H., S. Hong, and M. Kanamitsu, The NMC nested regional spectral model: An update, *Bull. Am. Meteorol. Soc.*, *78*, 2125–2143, 1997.

Kalnay, E., et al., The NCEP/NCAR 40-year Reanalysis project, *Bull. Am. Meteorol. Soc.*, *77*, 437–471, 1996.

Kanamitsu, M., Description of the NMC global data assimilation and forecast system, *Weather Forecasting*, *4*, 335–342, 1989.

Kanamitsu, M., W. Ebisuzaki, J. Woolen, J. Potter, and M. Fiorino, NCEP/DOE AMIP-II Reanalysis (R-2), *Bull. Am. Meteorol. Soc.*, *83*, 1631–1643, 2002.

Kida, H., T. Koide, H. Sasaki, and M. Chiba, A new approach for coupling a limited area model to a GCM for regional climate simulations, *J. Meteorol. Soc. Jpn.*, *69*, 723–728, 1991.

Kiehl, J. T., J. J. Hack, G. B. Bonan, B. A. Boville, D. L. Williamson, and P. J. Rasch, The National Center for Atmospheric Research Community Climate Model: CCM3, *J. Clim.*, *11*, 1131, 1998a.

Kiehl, J. T., J. J. Hack, G. B. Bonan, B. A. Boville, B. P. Briegleb, D. L. Williamson, and P. J. Rasch, Description of the NCAR Community Climate Model (CCM3), NCAR Tech. Note, *NCAR/TN-420 + STR*, 152 pp., Natl. Cent. for Atmos. Res., Boulder, Colo., 1998b.

Krishnamurti, T. N., A. Kumar, K. S. Yap, A. P. Dastoor, N. Davidson, and J. Sheng, Performance of high resolution mesoscale tropical prediction model, *Adv. Geophys.*, *32*, 133–286, 1990.

Lacis, A. A., and J. E. Hansen, A parameterization for the absorption of solar radiation in the Earth's atmosphere, *J. Atmos. Sci.*, *31*, 118–133, 1974.

Leung, L. R., and S. J. Ghan, Pacific Northwest climate sensitivity simulated by a regional climate model driven by a GCM: Part I. Control simulations, *J. Clim.*, *12*, 2010–2030, 1999a.

Leung, L. R., and S. J. Ghan, Pacific Northwest climate sensitivity simulated by a regional climate model driven by a GCM. Part II: 2 × CO_2 Simulations, *J. Clim.*, *12*, 2031–2053, 1999b.

Leung, L. R., A. F. Hamlet, D. P. Lettenmaier, and A. Kumar, Simulations of the ENSO hydroclimate signals in the Pacific Northwest Columbia river basin, *Bull. Am. Meteorol. Soc.*, *80*, 2313–2329, 1999.

Louis, J.-F., M. Tiedke, and M. Geleyn, A short history of the PBL parameterization at ECMWF, paper presented at ECMWF Workshop on Planetary Boundary Layer Parameterization, Eur. Cent. for Medium-Range Weather Forecasts, Reading, U.K., 1982.

Liu, Y., F. Giorgi, and W. M. Washington, Simulation of summer monsoon climate over East Asia with an NCAR regional climate model, *Mon. Weather Rev.*, *122*, 2331–2348, 1994.

Mearns, L. O., W. Easterling, C. Hays, and D. Marx, Comparison of agricultural impacts of climate change calculated from high and low resolution climate change scenarios: Part I. The uncertainty due to spatial scale, *Clim. Change*, *51*, 131–172, 2001.

McGregor, J. L., and K. J. Walsh, Climate change simulations of Tasmanian precipitation using multiple nestings, *J. Geophys. Res.*, *99*, 20,889–20,905, 1994.

Mesinger, F., and T. L. Black, On the impact of forecast accuracy of the step-mountain (eta) vs. sigma coordinate, *Meteorol. Atmos. Phys.*, *50*, 47–60, 1992.

Miller, N., and J. Kim, Numerical prediction of precipitation and river flow over the Russian River watershed during the January 1995 California storms, *Bull. Am. Meteorol. Soc.*, *77*, 101–105, 1996.

Nobre, P., A. D. Moura, and L. Sun, Dynamical downscaling of seasonal climate prediction over Nordeste Brazil with ECHAM3 and NCEP's regional spectral models at IRI, *Bull. Am. Meteorol. Soc.*, *82*, 2787–2796, 2001.

Perkey, D. J., Formulation of mesoscale numerical models, in *Mesoscale Meteorology and Forecasting*, edited by P. S. Ray, pp. 573–596, Am. Meteorol. Soc., Boston, Mass., 1984.

Pielke, R. A., *Mesoscale Meteorological Modeling*, 612 pp., Academic, San Diego, 1984.

Qian, J.-H., F. Giorgi, and M. S. Fox-Rabinovitz, Regional stretched grid generation and its application to the NCAR RegCM, *J. Geophys. Res.*, *104*, 6501–6513, 1999.

Roads, J. O., and S.-C. Chen, Surface Water and Energy Budgets in the NCEP Regional Spectral Model, *J. Geophys. Res.*, *105*, 29,539–29,549, 2000.

Roads, J. O., S.-C. Chen, and F. Fujioka, ECPC's weekly to seasonal global forecasts, *Bull. Am. Meteorol. Soc*, *82*, 639–658, 2001.

Roads, J., S.-C. Chen, and M. Kanamitsu, U.S. regional climate simulations and seasonal forecasts, *J. Geophys. Res*, in press, 2003.

Ropelewski, C., and M. Halpert, Global and regional scale precipitation patterns associated with the El Nino/Southern Oscillation, *Mon. Weather Rev.*, *115*, 1606–1626, 1987.

Schwarzkopf, M. D., and S. B. Fels, The simplified exchange method revisited: An accurate, rapid method for computation of infrared cooling rates and fluxes, *J. Geophys. Res.*, *96*, 9075–9096, 1991.

Soong, S.-T., and J.-W. Kim, Simulation of a heavy wintertime precipitation event in California, *Clim. Change*, *32*, 55–77, 1996.

Tackle, E. S., et al., Project to Intercompare Regional Climate Simulations (PIRCS): Description and initial results, *J. Geophys. Res.*, *104*, 19,443–19,461, 1999.

Troen, I., and L. Mahrt, A simple model of the atmospheric boundary layer: Sensitivity to surface evaporation, *Boundary Layer Meteorol.*, *37*, 129–148, 1986.

Uvo, C., C. Repelli, S. Zebiak, and Y. Kushnir, The relationships between tropical Pacific and Atlantic SST and Northeast Brazil Monthly Precipitation, *J. Clim.*, *11*, 551–562, 1998.

Xie, P., and P. A. Arkin, Global Precipitation: A 17-year Monthly Analysis Based on Gauge Observations, Satellite Estimates, and Numerical Model Outputs, *Bull. Am. Meteorol. Soc.*, *78*, 2539–2558, 1997.

Zhang, G. J., and N. A. McFarlane, Sensitivity, of climate simulations to the parameterizations of cumulus convection in the Canadian Climate Centre general circulation model, *Atmos. Ocean*, *33*, 407–446, 1995.

S. Chen and J. Roads, Experimental Climate Prediction Center, Scripps Institution of Oceanography, University of California, San Diego, 0224, La Jolla, CA 92023, USA. (jroads@ucsd.edu)

S. Cocke and T. LaRow, COAPS, Florida State University, Tallahassee, FL 32306, USA.

L. Druyan, M. Fulakeza, and P. Lonergan, Earth Institute at Columbia University and NASA/Goddard Institute for Space Studies, 2880 Broadway, New York, NY 10025, USA.

J.-H. Qian and S. Zebiak, International Research Institute, Lamont-Doherty Earth Observatory, Columbia University, Palisades, NY 10964, USA.